

Kinetico-Mechanistic Studies on a Reactive Organocopper(II) Complex: Cu-C bond Homolysis *versus* Heterolysis

Miguel A. González,^a Craig M. Williams,^a Manuel Martínez^{*b} and Paul V. Bernhardt^{*a}

^a School of Chemistry and Molecular Biosciences, University of Queensland, Brisbane 4072, Australia

^b Departament de Química Inorgànica i Orgànica, Secció de Química Inorgànica, Universitat de Barcelona, Martí i Franquès 1-11, and Institute of Nanoscience and Nanotechnology (IN2UB), Universitat de Barcelona, 08028 Barcelona, Spain

Abstract

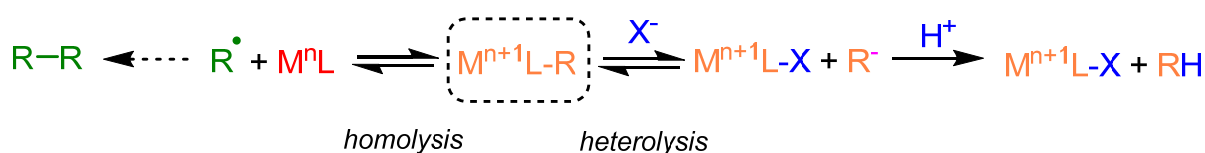
Organocopper(II) reagents are an unexplored frontier of copper catalysis. Despite being proposed as reactive intermediates, an understanding of the stability and reactivity of the Cu^{II}-C bond has remained elusive. Two main pathways can be considered for the cleavage mode of a Cu^{II}-C bond: homolysis, and heterolysis. We recently showed how organocopper(II) reagents can react with alkenes *via* radical addition, a homolytic pathway. In this work, the decomposition of the complex [Cu^{II}LR]⁺ (L = tris(2-dimethylaminoethyl)amine, Me₆tren, R = NCCH₂⁻) in the absence and presence of an initiator (RX, X = Cl, Br) was evaluated. When no initiator was present, first-order Cu^{II}-C bond homolysis occurred producing [Cu^IL]⁺ and succinonitrile from radical termination. When an excess of initiator was present, a subsequent formation of [Cu^{II}LX]⁺ via a second-order reaction was found, which results from the reaction of [Cu^IL]⁺ with RX following homolysis. However, when Brønsted acids (R'-OH: R' = H, Me, Ph, PhCO) were present, heterolytic cleavage of the Cu^{II}-C bond produced [Cu^{II}L(OR')]⁺ and MeCN. Kinetic studies were undertaken to obtain the thermal (ΔH^\ddagger , ΔS^\ddagger) and pressure activation parameters (ΔV^\ddagger), as well as deuterium kinetic isotopic effects, which provided an understanding of the strength of the Cu^{II}-C bond and the nature of the transition state for the reactions involved. These results reveal possible reaction pathways for organocopper(II) complexes relevant to their applications as catalysts in C-C bond forming reactions.

Introduction

Conceptually, the making or breaking of a metal-carbon bond can occur via multiple pathways, some of which involve changes in the formal oxidation state of the metal. In conventional organometallic chemistry well-known reactions such as oxidative addition and reductive elimination involve a 2-electron redox process linked to a change in coordination number of two. These reversible 2-electron and ligand reactions are at the heart of classic organometallic catalysts such as Wilkinson's hydrogenation catalyst, and the various Pd-catalyzed cross coupling reactions.¹ Although less common, related chemistry is possible for transition metals capable of reversible single electron redox reactions coupled to ligand complexation or dissociation; generally regarded as an atom transfer mechanism. In this case free radicals are necessarily involved.

The generic organometallic transition metal compound $M^{(n+1)}L-R$ may undergo metal-carbon bond dissociation following two different pathways (Scheme 1). Homolytic dissociation generates the corresponding one-electron reduced complex (M^nL) and an organic radical R^\bullet whereby the coordination number decreases by one. This reaction underpins organometallic mediated radical polymerization (OMRP)² where a controlled and reversible release of radicals through metal-carbon bond homolysis minimizes side reactions such as radical termination. Alternatively, heterolytic dissociation requires ligand substitution by an anionic species, X^- , which may be introduced in the form of its conjugate acid HX thus releasing RH ; a reaction commonly referred to as protonolysis. This is effectively an acid base reaction, and the oxidation state of the metal is unchanged.

In either case it is important to note that both the radical R^\bullet and carbanion R^- (a very strong base) cannot prevail in isolation so complexation as $LM^{(n+1)}-R$ stabilizes an otherwise highly reactive species.^{1,3} The polarity of the metal-carbon bond is essential to its reactivity. Alkyl complexes of high charge-density metal ions (Al^{3+} , Zn^{2+}) have a weakly stabilized $M-C$ bond, providing strong nucleophilicity and basicity of the alkyl group. Such complexes are typically highly sensitive to traces of water, leading to protonolysis of the $M-C$ bond (generating $M-OH$ and RH). Less electropositive metals afford more stable $M-C$ bonds such as in $[CH_3-HgL]^+$, which is quite stable to moisture and air.⁴



Scheme 1. Homolytic (left) and heterolytic (right) metal-carbon bond dissociation. Both processes are irreversible due to radical coupling (left) or HX being a stronger acid than RH (right).

Atom transfer radical polymerization (ATRP),⁵ and the closely related atom transfer radical addition (ATRA),⁶ reactions are further examples of transition metal catalyzed single electron atom

transfer reactions. Redox active Cu(II/I) complexes are at the forefront of ATRP/ATRA where halogen atom transfer at the Cu center is coupled to radical generation (Eqn. 1). We have shown that under electrochemically driven conditions where both the radical R[•] and Cu(I) complex are present, rapid radical capture can occur leading to an unusual organocopper(II) complex (Eqn. 2, k_{form}). This process abides by the same reversible bond homolysis reaction depicted in Scheme 1 and has parallels in the OMRP field, although Cu complexes are yet to find application in this area. While it has been noted that OMRP and ATRP mechanisms may occur synergistically in catalysis,⁷⁻⁹ the former reaction is only influenced by Cu^{II}-C bond reactivity.



In contrast to Cu(I), organocopper(II) reagents have remained largely unexplored in catalysis. Spectroscopically¹⁰⁻¹² or structurally¹³⁻¹⁵ characterized examples of organocopper(II) complexes are rare. Nevertheless, these compounds have been proposed as reactive intermediates formed by radical addition to a Cu(I) species in catalytic cycles (Eqn. 2).¹⁶⁻²⁰ Reactions between simple transition metal salts and radicals has a long history,²¹ but a clear picture of the stability and reactivity of the Cu^{II}-C bond and mechanistic analysis is lacking.

The reactivity of simple organocopper(II) complexes generated *in situ* by radicals formed by pulse radiolysis and Cu(I) precursors was investigated by Meyerstein and co-workers²²⁻²⁶ and a variety of mechanisms for Cu^{II}-C bond dissociation were considered. Ferraudi and co-workers observed that Cu(II) methylato complexes decompose by homolysis, and are less stable than the analogous carboxymethylato complexes.²⁷ These studies indicate that different co-ligand systems and alkyl radicals influence the decomposition pathway for the organocopper(II) complex in various ways. More recently, Matyjaszewski and co-workers generated the organometallic complex $[\text{Cu}^{\text{II}}(\text{TPMA})(\text{CH}_2\text{CN})]^+$ (TPMA = tris(2-pyridylmethyl)amine) in solution by mixing $[\text{Cu}^{\text{I}}(\text{TPMA})]^+$ with BrCH₂CN in a 2:1 ratio, which generated an equal mixture of $[\text{Cu}^{\text{II}}(\text{TPMA})\text{Br}]^+$ and $[\text{Cu}^{\text{II}}(\text{TPMA})(\text{CH}_2\text{CN})]^+$ as detected by UV-Vis spectroscopy.²⁸ A combination of Eqns 1 and 2 explains the formation of these two Cu(II) complexes. Decomposition of $[\text{Cu}^{\text{II}}(\text{TPMA})(\text{CH}_2\text{CN})]^+$ was studied at 25 °C, and occurred over a timescale of minutes to afford $[\text{Cu}^{\text{II}}(\text{TPMA})\text{Br}]^+$, with no accumulation of $[\text{Cu}^{\text{I}}(\text{TPMA})]^+$, indicating that the radical activation step (Eqn. 1) is rate limiting, while the subsequent radical capture (Eqn. 2) is fast ($k_{form} \gg k_{act}$).²⁹

In recent years we have utilized electrochemical and spectroscopic methods in tandem to generate a variety of organocopper(II) complexes based on both TPMA and its tertiary tetraamine analog tris(2-dimethylaminoethyl)amine (Me₆tren).¹⁰⁻¹² These studies have led to a reliable electrochemical method for generating $[\text{Cu}^{\text{II}}(\text{Me}_6\text{tren})(\text{CH}_2\text{CN})]^+$ in solution, which has been exploited

as a catalyst in electrochemical atom transfer radical addition (*e*ATRA) with high yields under mild conditions.³⁰

As this new C–C bond formation strategy is in its infancy, there is limited understanding of the reactivity of electrogenerated $[\text{Cu}^{\text{II}}(\text{Me}_6\text{tren})(\text{CH}_2\text{CN})]^+$ (hereafter $[\text{Cu}^{\text{II}}\text{LR}]^+$ for brevity: L = Me₆tren; R = NCCH₂[−]). To this end we herein report a full kinetic-mechanistic study of the Cu^{II}–C bond reactivity in $[\text{Cu}^{\text{II}}\text{LR}]^+$, including the influence of organic radicals and Brønsted acids, to gauge the relative importance of homolytic and heterolytic dissociation pathways.

Results and Discussion

As featured in Scheme 1, two main pathways can be considered for cleavage of the Cu^{II}-C bond: homolysis and heterolysis.³¹ As we have shown,³⁰ [Cu^{II}LR]⁺ reacts with alkenes *via* radical addition (Eqn. 3), which corresponds to a homolytic pathway. This leads to the loss of the visible absorption signals of [Cu^{II}LR]⁺, as colorless [Cu^IL]⁺ is formed when the stoichiometric reaction of [Cu^{II}LR]⁺ and alkenes concludes. When an excess of initiator (bromo- or chloroacetonitrile) was used, succinonitrile (NCCH₂CH₂CN or R-R) was also detected, again indicating homolysis of the Cu^{II}-C bond. Although all reactions are usually carried out under strictly anhydrous anaerobic conditions, when solvents were not completely anhydrous the final solution was pale blue, characteristic of Cu(II) species, and product yields were significantly lower. Nevertheless, the only products detected by ¹H NMR or GCMS were the radical addition termination products.



Contrary to expectations, [Cu^{II}LR]⁺ is relatively stable and can be manipulated in anaerobic solutions (MeCN) at room temperature over hour time-scales, but when exposed to moisture the product converted to a blue Cu(II) species instead. Previously we demonstrated that the Cu^{II}-CH₂CN bond is quite polarized, with a significant amount of the *d*-electron spin density delocalized over the cyanomethylato ligand from pulse EPR and DFT analysis,¹² which highlights the reactive character of this bond. Although the reaction pathways for the Cu^{II}-C bond are not well understood, Zhidomirov and co-workers have conducted DFT studies on alkyl-Cu(II) complexes with chlorido co-ligands, predicting a large bond dissociation energy of 40 kJ mol⁻¹ for homolysis.³² From our observations, two characteristics have to be considered with respect to the reactivity of the Cu^{II}-CH₂CN bond for the complex herein: lability (aligned with classical Cu(II) coordination chemistry), and competing homolysis. A series of kinetic studies were devised to fully understand the processes involved.

Homolysis pathway

The complex [Cu^{II}LR]⁺ was electro-generated in MeCN under anaerobic conditions, as described previously.³⁰ Only 1.1 equivalents of the initiator (XCH₂CN, X= Br, Cl) were present during the electrolysis, and the build-up of [Cu^{II}LR]⁺ was measured by its known electronic spectrum.^{10, 12} Once the formation of [Cu^{II}LR]⁺ was complete, the initiator RX was essentially consumed, thus limiting further radical activation with [Cu^IL]⁺ to produce [Cu^{II}LX]⁺ (Eqn. 1). From this point, different volumes of the [Cu^{II}LR]⁺ solution were diluted in anhydrous and degassed acetonitrile (always at 0.1 M (Et₄N)ClO₄ ionic strength after electrolysis) and the subsequent reaction was followed by time-resolved UV-Vis absorption spectroscopy. Under these conditions, formation of colorless *d*¹⁰ [Cu^IL]⁺ from green [Cu^{II}LR]⁺ was observed from the bleaching of the absorption bands at *ca.* 750, 620 and 400 nm (Figure 1). This observation, and the fact that succinonitrile (R-R) was a product, by ¹H NMR and GCMS

analysis, match the expected behavior from homolytic cleavage of the $\text{Cu}^{\text{II}}\text{-R}$ bond (Eqn. 2) and subsequent irreversible radical termination (Scheme 1, left).

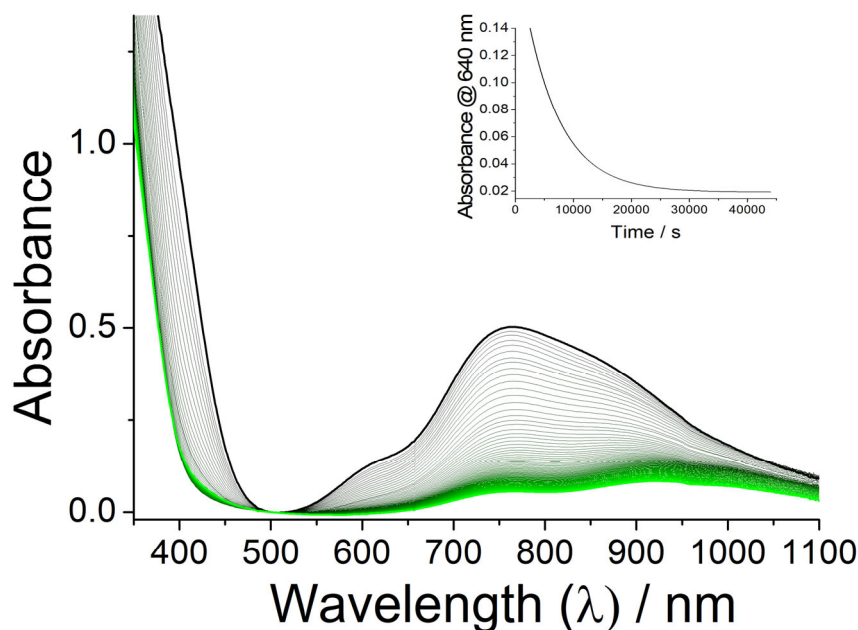


Figure 1. Time-resolved UV-Vis changes for the homolytic dissociation of $[\text{Cu}^{\text{II}}\text{LR}]^+$ (2 mM), $T = 45\text{ }^{\circ}\text{C}$. All peaks decrease in intensity with time. Note that the final spectrum (green) comprises $< 10\%$ of $[\text{Cu}^{\text{II}}\text{LBr}]^+$ as a side-reaction from residual BrCH_2CN with $[\text{Cu}^{\text{I}}\text{L}]^+$. Spectra collected every 60 s over a period of 12 h.

At high temperatures ($40\text{-}60\text{ }^{\circ}\text{C}$), the $[\text{Cu}^{\text{II}}\text{LR}]^+$ dissociation reaction followed a clean single first-order process that was modeled by the ReactLab Kinetics software.³³ The modeling was done with a final spectrum in Figure 1 that included a 10% amount of $[\text{Cu}^{\text{II}}\text{LBr}]^+$ ($\lambda_{\text{max}} \sim 950$ and 750 nm); due to the small excess of initiator RBr which reacted according to Eqn. 1. Furthermore, disproportionation of $[\text{Cu}^{\text{I}}\text{L}]^+$ (Eqn. 4) becomes a competitive side reaction at longer reaction times ($>12\text{ h}$), which were avoided. The formation of a precipitate due to elemental Cu was most apparent at lower temperatures and high total copper concentration ($> 2\text{ mM}$), conditions that were consequently also avoided. In fact, rapid disproportionation of $[\text{Cu}^{\text{I}}\text{L}]^+$ has been observed in aqueous solution and has been exploited for catalytic single-electron transfer living radical polymerization (SET-LRP);³⁴⁻³⁶ in acetonitrile solution this process is not fast enough to induce living radical polymerization.³⁷⁻³⁸



The homolytic decomposition rate of $[\text{Cu}^{\text{II}}\text{LR}]^+$ at different concentrations between $40\text{ }^{\circ}\text{C}$ and $60\text{ }^{\circ}\text{C}$ did not exhibit a dependence on the $\text{Cu}(\text{II})$ concentration. Although, bimolecular reductive elimination has been proposed as a bond cleavage pathway (Eqn. 5, which is second order with respect to $[\text{Cu}^{\text{II}}\text{LR}]^+$), experiments disclosed herein could not confirm this reaction given the lack of dependence

of k_{obs} on $[Cu^{II}]$ over the concentration range examined. As a result, the first order rate constant was assigned to Eqn. 2 (reverse reaction) with a value at 40 °C of $k_{homol} = 3.2 \times 10^{-5} \text{ s}^{-1}$ ($t_{1/2} \sim 6 \text{ h}$), $[Cu^{II}LR]^+$ acting as a persistent source of organic radicals.³⁹



An alternate reaction that may be taking place is catalyzed radical termination (CRT, Eqn. 6), a bimolecular process where $[Cu^{II}LR]^+$ reacts with another radical R' to form the termination product $R-R'$ and $[Cu^IL]^+$. Studies on homolytic bond cleavage of different organometallic species have shown that stable radicals such as 2,2,6,6-tetramethylpiperidin-1-oxyl (TEMPO) can induce homolytic bond cleavage with a reaction that is linearly dependent on radical concentration. The influence of $[TEMPO]$ on the observed rate constant for the homolytic decomposition of $[Cu^{II}LR]^+$ at 40 °C was studied under pseudo first order conditions resulting in the adduct TEMPO-R (Scheme 2). The experiments showed that $[Cu^IL]^+$ is the final copper-containing product, and the observed first order rate constants ($k_{obs,TEMPO}$) exhibit a linear dependence on $[TEMPO]$ (Figure 2). From these data fit to Eqn. 7 the bimolecular rate constant $k_{TEMPO} = 5.3 \times 10^{-2} \text{ M}^{-1} \text{ s}^{-1}$ at 40 °C was obtained from the slope, while the small intercept (k_{homol}) agrees strongly with the value determined in the absence of TEMPO indicated above.

$$k_{obs,TEMPO} = k_{TEMPO}[TEMPO] + k_{homol} \quad (\text{Eqn. 7})$$

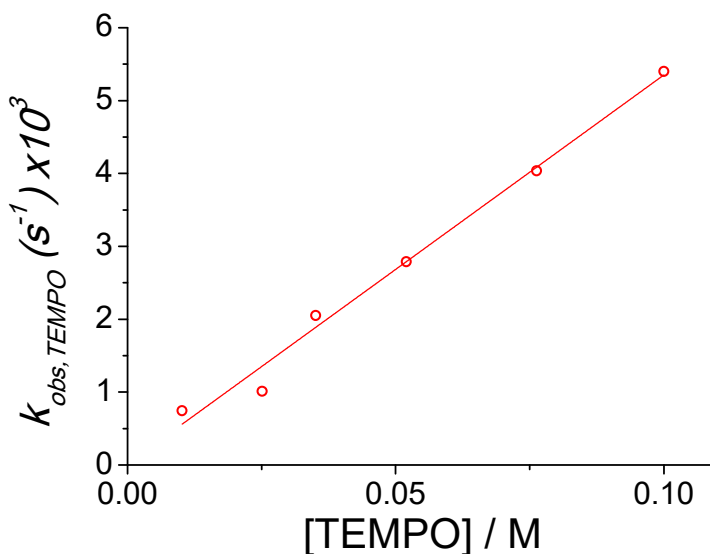
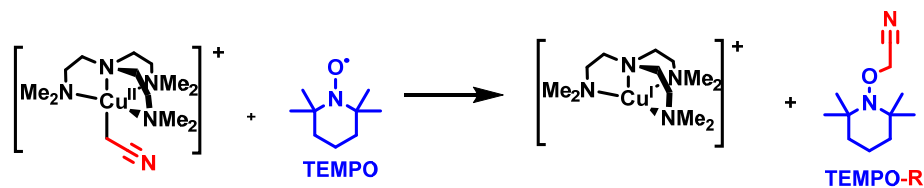


Figure 2. Linear dependence of $k_{obs,TEMPO}$ with $[TEMPO]$ for the homolytic decomposition of $[Cu^{II}LR]^+$ via catalyzed radical termination. 40 °C, dry anaerobic MeCN.

The stoichiometric reaction of TEMPO with $[Cu^{II}LR]^+$ was also conducted and after workup (Experimental Section) ^1H NMR (Supporting Information, Figure S1) and GC-MS analysis, confirmed

formation of the TEMPO-R adduct that has been reported from the reaction of cyanomethyl radicals with TEMPO.⁴⁰ Only small amounts of succinonitrile were formed.



Scheme 2. Radical termination reaction with TEMPO.

These results show that CRT (Eqn. 6) is indeed a possible pathway for homolytic bond dissociation. However, this does not imply that the formation of $[\text{Cu}^{\text{I}}\text{L}]^+$ and R-R (succinonitrile) in the absence of TEMPO (Figure 1) follows the same pathway, i.e. $[\text{Cu}^{\text{II}}\text{LR}]^+$ reacting directly with $\text{R}\cdot$. In this respect, when additional equivalents of the RX initiator ($\text{X} = \text{Br}, \text{Cl}$) were added to the initial reacting solutions of $[\text{Cu}^{\text{II}}\text{LR}]^+$, the final product was $[\text{Cu}^{\text{II}}\text{LX}]^+$ (Figure 3). In this case, the kinetic profiles are biphasic, and the two steps could be easily resolved. The slower step leads to $[\text{Cu}^{\text{I}}\text{L}]^+$ with no absorption in the 500-1100 nm region, while the faster step produces $[\text{Cu}^{\text{II}}\text{LX}]^+$. In Figure 4 the spectrum of the final product is $[\text{Cu}^{\text{II}}\text{LBr}]^+$, with its characteristic absorption maxima at *ca.* 970 and 750 nm,¹⁰ produced by the atom transfer reaction (Eqn. 1), which is made irreversible by radical termination.⁴¹ Note that the fact that the $[\text{Cu}^{\text{I}}\text{L}]^+$ is produced more slowly than its consumption by the RX initiator prevents its buildup and avoids the requirement to use large concentration of RX to reach pseudo-first order conditions.

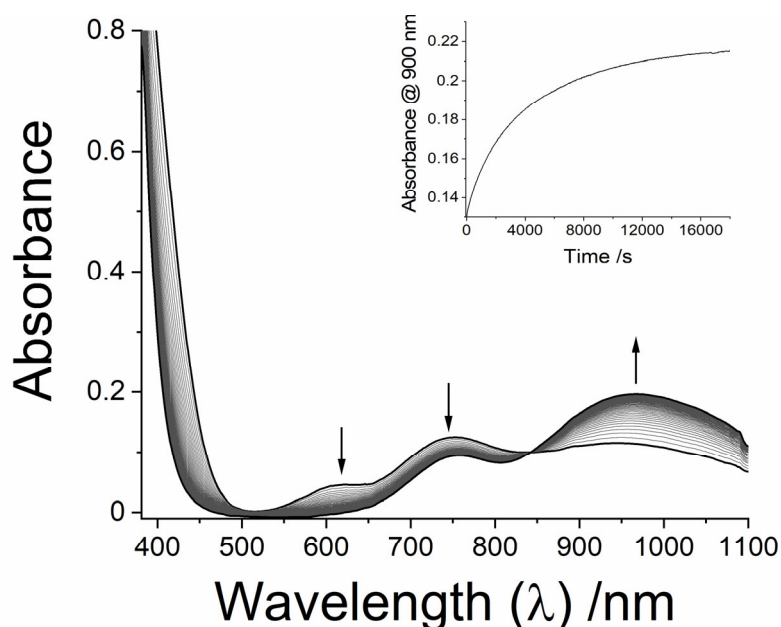


Figure 3. Time-resolved UV-Vis changes for a 1 mM solution of $[\text{CuL}(\text{CH}_2\text{CN})]^+$ and 2.0 mM BrCH_2CN (added after formation of $[\text{CuL}(\text{CH}_2\text{CN})]^+$), anaerobic conditions. $T = 25^\circ\text{C}$. Spectra recorded every 60 s for ~5 h.

The dependence of the observed rate constants for the fast and slow processes on [RX] was determined, and the data are shown in Figure 5. As expected, the slower step $k_{obs,1}$ is independent of [RX] and its value is within experimental error of the $[\text{Cu}^{\text{II}}\text{LR}]^+$ homolysis rate constant determined above ($k_{obs,1} = k_{homol} = 1.1 \times 10^{-5} \text{ s}^{-1}$ at 30 °C). However, for the faster step $k_{obs,2}$ a linear dependence on [RX] was observed, and the slopes of these lines provide the activation rate constants for Eqn. 1 (forward reaction) where $k_{act-X} = k_{obs,2} / [\text{RX}]$. The values of k_{act-X} ($X = \text{Cl}, \text{Br}$) for this system with chloro- and bromoacetonitrile have been reported previously,⁴² and the values obtained herein are of the same order of magnitude. As expected, the $k_{act-\text{Br}}$ and $k_{act-\text{Cl}}$ second-order rate constants differ by an order of magnitude, based on their bond dissociation energies (see Table 1).

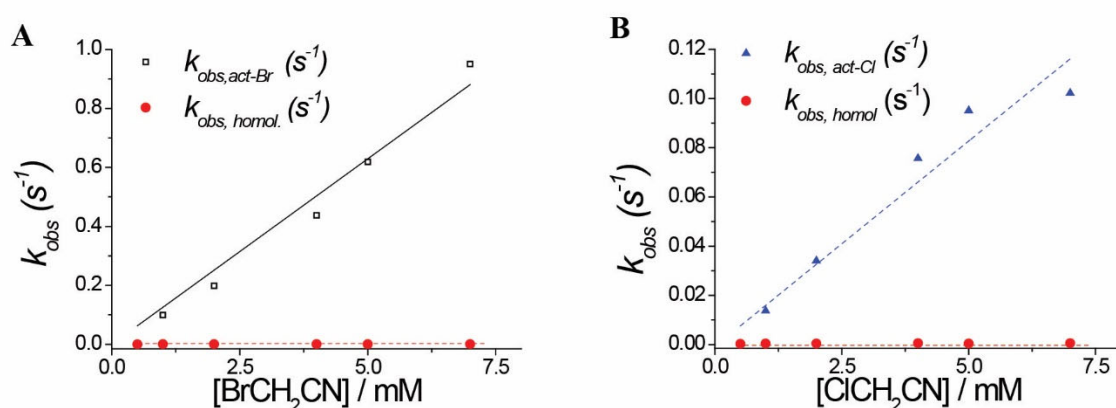


Figure 4. Trends of observed rate constants (k_{obs}) with [RX] ($X = \text{Br}$, **A**; Cl , **B**) at 25 °C.

The temperature dependence of the k_{homol} and k_{act-X} rate constants allowed an evaluation of the enthalpies (ΔH^\ddagger) and entropies (ΔS^\ddagger) of activation from standard Eyring plots (Figure 5, Eqn. S1). Similarly, from standard $\ln k$ vs P plots (Figure 6, Eqn. S2) the volumes of activation were determined. (Table 1).

Table 1. Thermal and pressure activation parameters for the $[\text{Cu}^{\text{II}}\text{LR}]^+$ homolysis and halogen atom transfer reactions.

	Homolysis	Atom Transfer X=Br	Atom Transfer X=Cl
$k_{homol} \text{ (s}^{-1}\text{) (323 K)}$	1.8×10^{-4}	–	–
$k_{act-X} \text{ (M}^{-1} \text{ s}^{-1}\text{) (303 K)}$	–	1.5×10^2	1.7×10^1
$\Delta H^\ddagger \text{ (kJ mol}^{-1}\text{)}$	$+113 \pm 7$	$+40 \pm 4$	$+60 \pm 7$
$\Delta S^\ddagger \text{ (J mol}^{-1} \text{ K}^{-1}\text{)}$	$+30 \pm 20$	-78 ± 13	-34 ± 22
$\Delta V^\ddagger \text{ (cm}^3 \text{ mol}^{-1}\text{)}$	$+8 \pm 1$	$+26 \pm 3$	n.d.

For the homolysis reaction (reverse of Eqn. 2 i.e. k_{homol} with no initiator present), ΔH^\ddagger is large and reflects the resistance of the $\text{Cu}^{\text{II}}-\text{CH}_2\text{CN}$ bond to homolytic cleavage, which is consistent with our observations on the electro-generation of the complex. Given the fact that the reverse formation of $[\text{Cu}^{\text{I}}\text{LR}]^+$ (Eqn. 2) occurs at close to diffusion-limited rates,¹⁰ the corresponding ΔH^\ddagger value must be very small ($<2 \text{ kcal mol}^{-1}$),⁴³⁻⁴⁴ which suggests that the value determined here for the ΔH^\ddagger of homolysis is close to the $\text{Cu}^{\text{II}}-\text{CH}_2\text{CN}$ bond dissociation energy (BDE).⁴⁵ Although there are no thermodynamic data on the bond homolysis of organocopper(II) complexes, for other metals, such as Co(III) with salen (*N,N'*-ethylenebis(salicylimine)), the BDE is within the range $80\text{-}170 \text{ kJ mol}^{-1}$.⁴⁶ The small positive value of ΔS^\ddagger indicate a slight increase of disorder in the transition state, since two species (R^\cdot and $[\text{Cu}^{\text{I}}\text{L}]^+$) are emerging from one entity. The values of ΔV^\ddagger report on changes in volume between the transition state and the reactants, and therefore on the structure of the transition state itself.⁴⁷ From Figure 6A a slight decrease of the rate constant on increasing pressure was found to give $\Delta V^\ddagger = 8 \pm 1 \text{ cm}^3 \text{ mol}^{-1}$ (Table 1), which was expected from the partial dissociation of The Cu–C bond in the transition state $\{[\text{LCu}\cdots\text{R}]^+\}^\ddagger$.

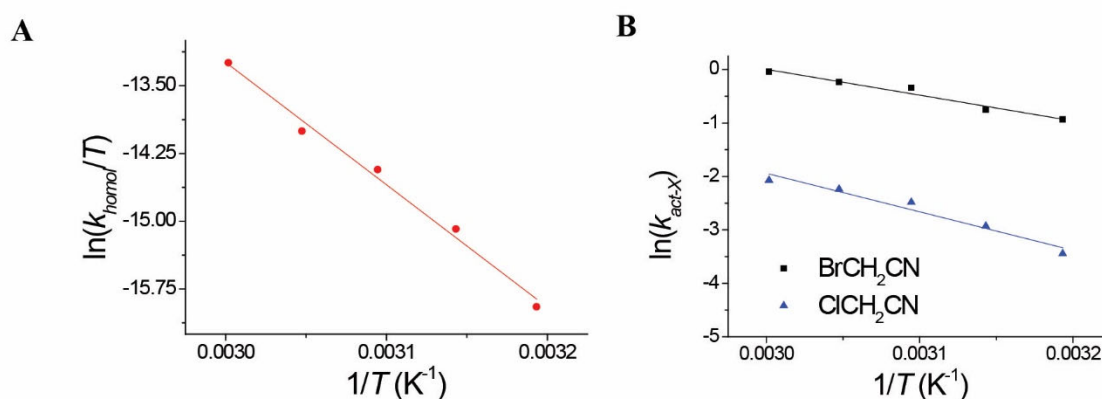


Figure 5. (A) Eyring plots for the homolysis step (k_{homol}), and (B) for the halogen atom transfer (k_{act-X}) reaction.

For the reaction carried out in the presence of RX initiator, i.e. atom-transfer radical activation (k_{act-X}), the increase observed in ΔH^\ddagger on going from $X = \text{Br}$ to Cl reflects the increased BDE of the C–Cl bond going to the transition state coupled with a greater affinity of the $[\text{Cu}^{\text{I}}\text{L}]^+$ complex for the incoming Br atom. The negative value of ΔS^\ddagger was expected given the high ordering needed to form the transition state, i.e. $\{[\text{LCu}\cdots\text{X}\cdots\text{R}]^+\}^\ddagger$. Furthermore, the value of ΔV^\ddagger (Figure 6B) shown in Table 1 was much more positive than that determined for k_{homol} , which again indicates a significant expansion of the transition state $\{[\text{LCu}\cdots\text{Br}\cdots\text{R}]^+\}^\ddagger$ assembly.

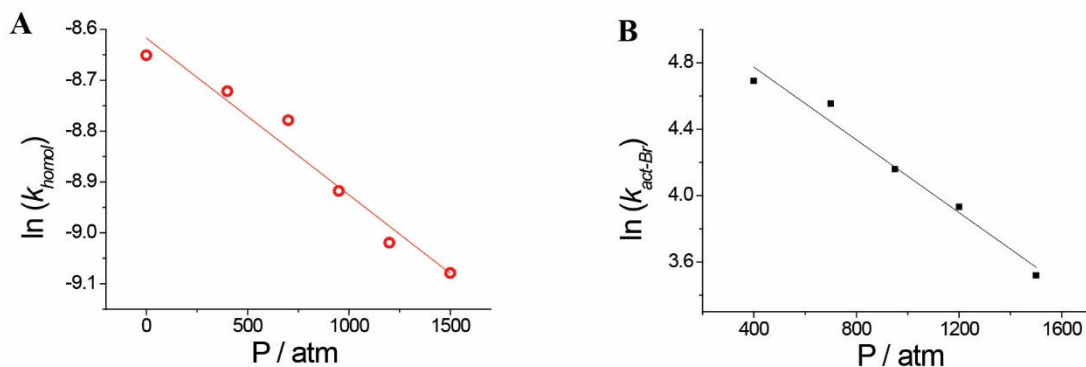


Figure 6. Plots of $\ln k$ vs P for (A) the homolytic bond dissociation reaction at 40 °C, and for (B) the atom transfer activation with bromoacetonitrile, at 25 °C.

Heterolysis (Protonolysis) Pathway

To date there has been no evidence that $[\text{Cu}^{\text{II}}\text{LR}]^+$ undergoes spontaneous heterolytic $\text{Cu}^{\text{II}}-\text{C}$ bond cleavage. The addition of an electrophile, such as benzaldehyde, to electro-generated $[\text{Cu}^{\text{II}}\text{LR}]^+$ in CH_3CN did not lead to any products expected from nucleophilic attack by R^- , a reaction which takes place readily for organocopper(I) complexes. Therefore, conventional heterolysis, releasing the cyanomethylate anion R^- and $[\text{Cu}^{\text{II}}\text{L}]^+$, is non-competitive with homolysis under these conditions. Nevertheless, when samples of $[\text{Cu}^{\text{II}}\text{LR}]^+$ in MeCN contained equimolar amounts of H_2O , the final product was a pale-blue Cu(II) species, suggesting a heterolytic protonolysis pathway (hydrolysis) (Figure 7). This observation matches the heterolytic decomposition previously observed by Meyerstein *et al.* for transient organocopper(II) complexes formed in aqueous solution.^{23, 26, 48} Consequently, the reactivity of $[\text{Cu}^{\text{II}}\text{LR}]^+$ in MeCN under anaerobic conditions with different concentrations of H_2O (0.7–4.4 M, pseudo-first-order conditions at 0.1 M $(\text{Et}_4\text{N})\text{ClO}_4$) was investigated. In all experiments a single first order process was observed, and the data were modelled with ReactLab Kinetics³³ according to the reaction depicted in Eqn. 8 producing a pseudo-first-order rate constant $k_{\text{obs,prot}}$ for each experiment. As the cyanomethylate anion ($\text{NCCH}_2^- = \text{R}^-$) is a strong base ($\text{p}K_{\text{a}}$ of 31.3 in DMSO),⁴⁹ the products of the reaction must be MeCN and $[\text{Cu}^{\text{II}}\text{L}(\text{OH})]^+$. The final spectrum effectively showed a broad band at ca. 870 nm, and a shoulder at 680 nm, which corresponds to the known hydroxido complex $[\text{Cu}^{\text{II}}\text{L}(\text{OH})]^+$.⁵⁰



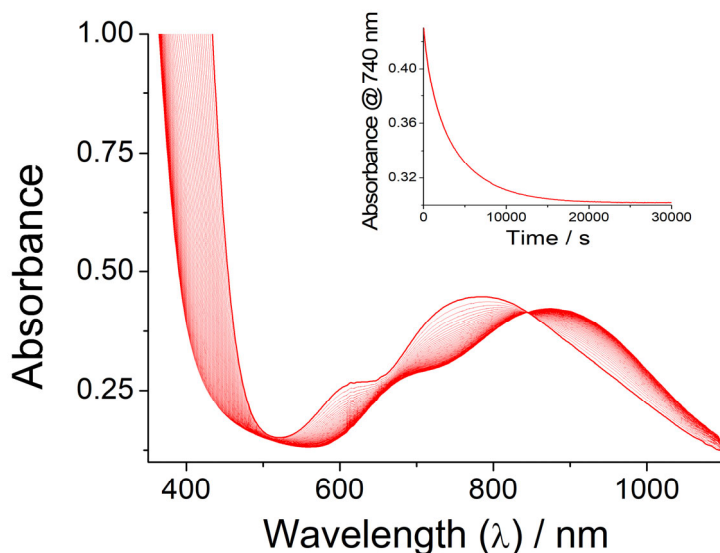


Figure 7. Time-resolved UV-Vis changes for a 2 mM solution of $[\text{CuLR}]^+$ in the presence of water (2 M). $T = 40^\circ\text{C}$.

Interestingly, at low $[\text{H}_2\text{O}]$ values, a contribution of the slower homolysis reaction was observed, indicated by a diminution, rather than a shift, of the Cu(II) absorption bands over time. Clearly, a competition between the two bond cleavage pathways was occurring at low water concentrations. Similarly, alkylchromium(III) complexes have been shown to undergo homolytic $\text{Cr}^{\text{III}}\text{--C}$ bond cleavage and hydrolysis⁵¹ in a competing manner, with factors such as the ligand choice or reaction conditions favoring the bond cleavage towards one pathway.⁵²⁻⁵³

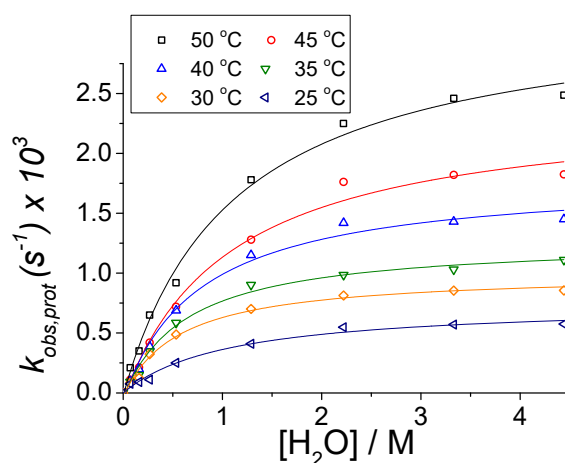
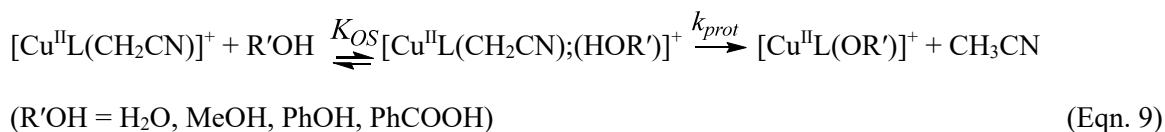


Figure 8. Dependence of the pseudo-first-order rate constant for the protonolysis process, $k_{\text{obs,prot}}$, of $[\text{Cu}^{\text{II}}\text{LR}]^+$ on $[\text{H}_2\text{O}]$.

The dependence of $k_{\text{obs,prot}}$ on $[\text{H}_2\text{O}]$ (Figure 8) showed the expected behavior described by an Eigen-Wilkins mechanism,⁵⁴ where a rapid pre-equilibrium forms an outer-sphere (OS) encounter complex that leads, via the rate determining step, to the final complex (Eqn. 9). The values of K_{OS} (average for all temperatures) and k_{prot} derived from fitting the data to Eqn. 10 are collected in Table 2. Evidently, the organocopper(II) complex $[\text{Cu}^{\text{II}}\text{LR}]^+$ is remarkably stable to hydrolysis, relative to most

polar organometallics, with a half-life of *ca.* 84 min at 35 °C at high [H₂O] values, which reinforces our earlier study whereby [Cu^{II}(TPMA)(CH₂CN)]⁺ is still formed electrochemically even in the presence of added water.¹⁰



$$k_{\text{obs,prot}} = \frac{k_{\text{prot}}K_{\text{OS}}[\text{R}'\text{OH}]}{1+K_{\text{OS}}[\text{R}'\text{OH}]} \quad (\text{Eqn. 10})$$

The dependence of the values of k_{prot} on temperature and pressure were analyzed by standard Eyring (Figure S2) and $\ln k$ vs P plots (Figure S4A), and the values of ΔH^\ddagger , ΔS^\ddagger and ΔV^\ddagger were derived (Table 2). While the large negative value of ΔS^\ddagger indicates a mechanism where the incoming water molecule and the complex should be associated in the transition state, the modest value of ΔH^\ddagger indicates that the process is not very energy demanding. This is expected for associative mechanisms where a higher degree of bond-forming than bond-breaking occurs going to the transition state.⁵⁵ As for the volume of activation, ΔV^\ddagger , the value distinctly indicates an expansion on going to the transition state, which is in agreement with an incoming water molecule and a departing MeCN group within the transition state structure.

Equivalent protonolysis reactions were carried out with a series of organic acids with different $\text{p}K_{\text{a}}$ values (methanol, phenol, and benzoic acid) under the same conditions. In all cases, the same behavior following Eqn. 9 was observed (Figures S3 and S4), and the relevant kinetic and activation parameters are provided in Table 2. Interestingly, as the substrate $\text{p}K_{\text{a}}$ decreases the value of k_{prot} increases significantly, the maximum being for benzoic acid, which required working at lower temperatures to obtain reproducible rate constants under standard mixing conditions. Similarly, higher values of K_{OS} were associated with the more acidic proton donors, i.e. lower concentrations were required to reach the saturation value of $k_{\text{obs,prot}}$ (Eqn. 10). These results highlight the importance of proton donation and hydrogen bonding in forming the outer-sphere complex, and in the overall reaction kinetics.

As seen in Table 2, a decrease in the values of ΔH^\ddagger was observed with increasing proton donor acidity, which indicates that reaching the transition state is less energetically demanding when O–H bond breaking is facilitated. Concurrently, ΔS^\ddagger becomes more negative with increasing proton donor acidity *i.e.* an increased ordering of transition state relative to the reactants. As for the values of ΔV^\ddagger (determined at 4 M water concentration, where saturation kinetics conditions have been reached), they indicate a greater expansion going to the transition state with increasing Brønsted acidity and molar volume of the proton donor, which suggests a late transition state. The positive values of ΔV^\ddagger (expansion of the transition state) and the negative values of ΔS^\ddagger (ordering of the transition state) agree

with a mechanism where intermolecular interactions are significant within the transition state. These phenomena are well-known in the literature, with examples such as hydrogen bonding being an important contribution to these values of ΔV^\ddagger .⁵⁶⁻⁵⁷ The significance of the activation parameters will be further discussed on proposing a general structure for the transition state.

Table 2. Kinetic and thermal and pressure activation parameters for the protonolysis reaction of $[\text{Cu}^{\text{II}}\text{LR}]^+$ with different acidic species in MeCN. ‘318’ superscripts denote the temperature (K).

	Methanol	Water	Phenol	Benzoic Acid
$\text{p}K_{\text{a}}$	15.3	14.0	10.0	4.2
ΔH^\ddagger (kJ mol ⁻¹)	+68±4	+64±2	+53±4	+43±3
ΔS^\ddagger (J K ⁻¹ mol ⁻¹)	-90±15	-83±6	-130±12	-150±9
ΔV^\ddagger (cm ³ mol ⁻¹)	18±1	14±1	22±2	34±3
KIE (³¹⁸ $k_{\text{obs,protH}}/k_{\text{obs,protD}}$)	1.5	2.2	2.6	n.d.
³¹⁸ K_{OS} (M ⁻¹)	2±1	1.1±0.2	23±11	55±14
³¹⁸ k_{prot} (s ⁻¹)	5.2×10^{-4}	8.5×10^{-4}	7.3×10^{-4}	3.9×10^{-3}

Given the importance of proton donation and hydrogen bonding in the mechanism observed for this process, an evaluation of the deuterium kinetic isotopic effect (KIE) was pursued. When the protonolysis reaction was carried out with D₂O, the observed reaction rate under saturation kinetics conditions, $k_{\text{prot(D)}}$, was significantly slower than with H₂O as is apparent in Figure 9. A primary kinetic isotope effect $\text{KIE} = k_{\text{H}}/k_{\text{D}}$ of 2.2 was obtained, indicating that bond breaking involving O–H is indeed dominant in the rate-limiting step. Equivalent KIEs for MeOH/MeOD and PhOH/PhOD were 1.5, and 2.6, respectively which follows the same trend as the Brønsted acidity of the proton donor, the stronger acids leading to a greater KIE.

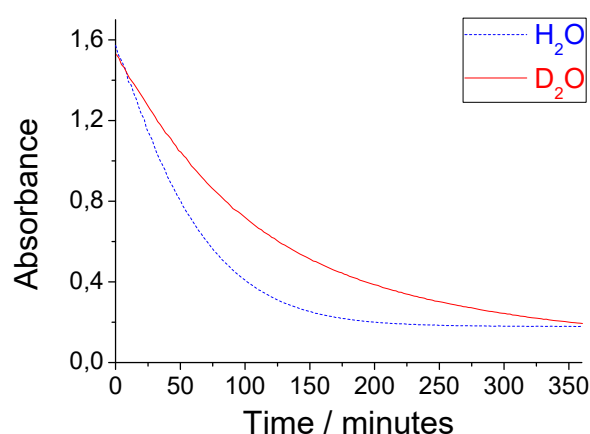
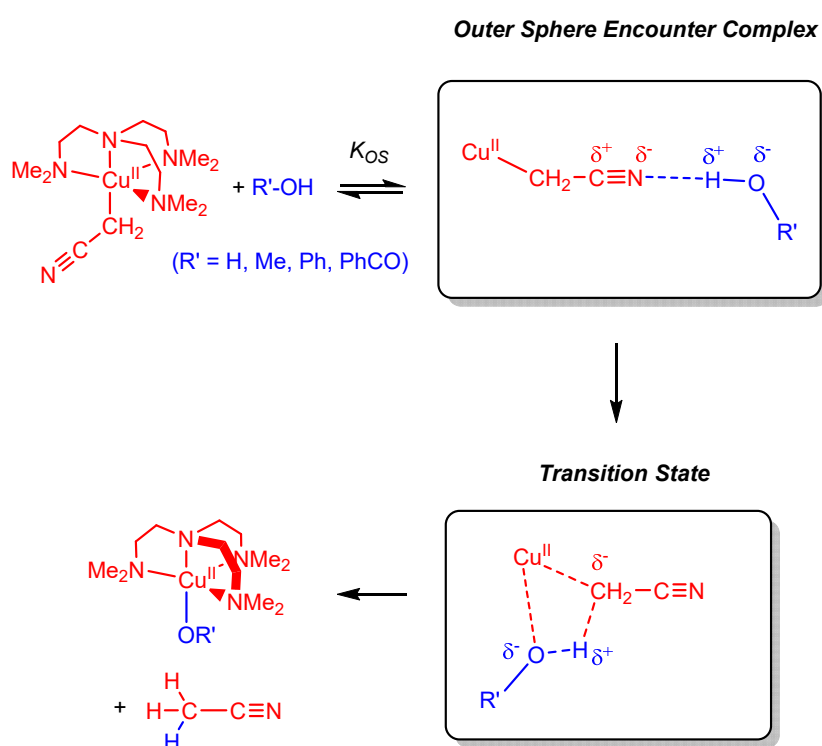


Figure 9. Absorbance (at 370 nm) vs time for the protonolysis/deuterolysis of $[\text{CuLR}]^+$ carried out in H₂O (blue dotted line) and D₂O (red solid line) at 40 °C.

Characterization of the product MeCN from $[\text{Cu}^{\text{II}}\text{LR}]^+$ protonolysis was pursued to confirm that the NCCH_2^- ligand is the site of protonation. Given that the product is the same as the solvent,

isotopic labelling was necessary. The reaction was performed on a quantitative scale (see Experimental Section) using a 10-fold excess of D₂O, and the product was analyzed by ²H NMR spectroscopy. The product is indeed acetonitrile-*d*₁ (CDH₂CN), as characterized by ²H NMR of the reaction mixture, where a triplet at 1.9 ppm with ²J_{H-D} = 2.3 Hz is observed (Figure S5).

In summary, based on the thermal and pressure activation parameters (Table 2), and the presence of a significant KIE, the mechanism indicated in Scheme 3 is proposed for the protonolysis reaction of [Cu^{II}LR]⁺. An alternative mechanism involving an associative process via a hexacoordinated {LCu^{II}-(HOR')R} intermediate is considered unlikely; there are more than 80 crystal structures of transition metal complexes of the sterically bulky Me₆tren ligand in the Cambridge Structural Database and none have a coordination number greater than five.



Scheme 3. Proposed reaction mechanism for the protonolysis (heterolysis) of [Cu^{II}LR]⁺ (L = Me₆tren, R = NCCH₂⁻) in presence of a Brønsted acid R'OH (R' = H, Me, Ph, PhCO).

The increase in *K*_{OS} with R'OH acidity (Table 2) indicates that the -OH functional group is involved in non-covalent bonding within the outer sphere complex and the terminal nitrile N-atom of [Cu^{II}LR]⁺ is the only possible proton acceptor. Progression to the transition state is expected with significant negative values of Δ*S*[‡] that indicate a higher ordering for the reactions with stronger acids. This fact is related to an increase in the later nature of the transition state, which correlates with an increase of the value determined for the deuterium KIE. The values of the activation volumes Δ*V*[‡] show an expansion increase for the same sequence, which seems to be contrary to the trend in the values of

the activation entropy. However, the late transition state involving a significant proton dissociation KIE >1 and a consequent $\text{Cu}^{\text{II}}-\text{CH}_2\text{CN}$ breakage is consistent with an expansion of the system. In fact, for cyclometallation reaction studies on Pd(II) and Rh(II) complexes, which can be considered mechanistically relevant to the reverse of the reaction studied here, the values of ΔV^\ddagger are clearly negative.⁵⁸⁻⁶⁰

Conclusions

This work has shown that $\text{Cu}^{\text{II}}-\text{C}$ bond dissociation in the organocopper(II) complex $[\text{Cu}^{\text{II}}\text{LR}]^+$ ($\text{L} = \text{Me}_6\text{tren}$, $\text{R} = \text{NCCH}_2^-$) may occur either homolytically (to give $[\text{Cu}^{\text{I}}\text{L}]^+$ and R^\bullet) or heterolytically in the presence of a Brønsted acid $\text{R}'\text{OH}$ (to give $[\text{Cu}^{\text{II}}\text{L}(\text{OR}')^+]$ and RH). This represents the first study reporting thermal and volume activation parameters for this emerging class of organocopper(II) complexes. From these studies, distinct modes of reactivity are found possible depending on the substrate present.

In neat MeCN, under anaerobic conditions at 0.1 M $(\text{Et}_4\text{N})\text{ClO}_4$, $[\text{Cu}^{\text{II}}\text{LR}]^+$ has a half-life of approximately 6 h, and a dominant pathway of homolysis of the $\text{LCu}^{\text{II}}-\text{CH}_2\text{CN}$ bond is followed by irreversible radical dimerization ($2 \text{ }^\bullet\text{CH}_2\text{CN} \rightarrow \text{NCCH}_2\text{CH}_2\text{CN}$) to give $[\text{Cu}^{\text{I}}\text{L}]^+$. When XCH_2CN ($\text{X} = \text{Br}, \text{Cl}$) is introduced, two reactions occur sequentially; (i) homolysis and (ii) halogen atom transfer between $[\text{Cu}^{\text{I}}\text{L}]^+$ and XCH_2CN leading to $[\text{Cu}^{\text{II}}\text{LX}]^+$ (and $^\bullet\text{CH}_2\text{CN}$) with k_{act-X} values that match published data. For simple homolysis, the large positive ΔH^\ddagger value found indicated a strong $\text{Cu}^{\text{II}}-\text{C}$ coordinate bond, and the positive ΔS^\ddagger and ΔV^\ddagger values are as expected for this formal dissociation reaction. For the activation step of atom transfer, the ΔH^\ddagger values reflected differences in $\text{C}-\text{X}$ bond dissociation energies in chloro- and bromoacetonitrile while negative ΔS^\ddagger and positive ΔV^\ddagger values are consistent with an ordered and expanded transition state of the type $\{[\text{LCu}\cdots\text{X}\cdots\text{CH}_2\text{CN}]^+\}^\ddagger$ being formed.

In contrast to homolysis, there is no evidence that heterolysis of the $\text{LCu}^{\text{II}}-\text{CH}_2\text{CN}$ bond (to yield $\text{Cu}^{\text{II}}\text{L}$ and NCCH_2^-) occurs spontaneously. Instead, NCCH_2^- substitution must be triggered by a Brønsted acid such as water, methanol, phenol or benzoic acid leading to the release of the conjugate acid MeCN. For all proton donors studied the protonolysis reaction followed an Eigen-Wilkins mechanism involving formation of an intermediate outer-sphere complex, with an equilibrium constant (K_{os}) increasing with the proton donor acidity. The observed trends of positive ΔV^\ddagger and negative ΔS^\ddagger for the protonolysis rate constant also indicated that the proton donor strength is a determining factor in ordering and expanding the reactants within the transition state of the reaction. Moreover, significant deuterium isotope effects were observed, confirming that $\text{O}-\text{H}$ bond breaking plays a key role.

Overall, the studies carried out herein demonstrate that although the $\text{LCu}^{\text{II}}-\text{CH}_2\text{CN}$ bond is strong it is highly reactive, resulting in these complexes being sufficiently robust but suitably labile for

homogeneous catalysts in C–C bond forming reactions (e.g. electrochemical atom transfer radical addition).

Experimental Section

Reagents

The reaction conditions for electrochemical generation of $[\text{Cu}^{\text{II}}\text{LR}]^+$ have been described in great detail in a previous article.³⁰ All solvents were dried by distillation from CaH_2 and stored in activated 3 Å molecular sieves. All solvents were HPLC grade. Both alkyl halide initiators, BrCH_2CN and ClCH_2CN , were commercially available and were used without further purification. The inert electrolyte $(\text{Et}_4\text{N})\text{ClO}_4$ was prepared and recrystallized as previously described.¹⁰ Reactions were performed anaerobically to prevent rapid oxidation of $[\text{Cu}^{\text{I}}\text{L}]^+$ to $[\text{Cu}^{\text{II}}\text{LX}]^+$ with Schlenk techniques, using N_2 or Ar as the inert gas; alternatively, solutions were prepared in a glovebox ($\text{O}_2 < 20$ ppm). The radical 2,2,6,6-tetramethylpiperidin-1-oxyl (TEMPO) was used as received and no further purification was made.

Kinetic Experiments and Instrumentation

Reactions were carried out in CH_3CN , at $I = 0.1$ M $(\text{Et}_4\text{N})\text{ClO}_4$. All homolysis experiments were kept at or below 2 mM to avoid side-reactions. The temperatures used for the spontaneous homolysis reaction (Eqn. 9) were in the 40-60 °C range; lower temperatures also led to side-reactions. For this reaction, the concentration of initiator was assumed to be negligible since 1.1 equivalents of XCH_2CN were used, which were essentially completely consumed. The reactions with TEMPO were studied at 40 °C. The reactions with excess initiator were studied between 25-45 °C: the concentration of $[\text{Cu}^{\text{II}}\text{LR}]^+$ was kept at 1 mM, and the variable concentrations of initiator (Br or ClCH_2CN) were in the range of 0.5-7.0 mM.

Kinetic experiments were performed with an Agilent HP 8453 diode array UV-Vis spectrophotometer, equipped with a thermostatted (± 0.1 °C) multicell transport. A CARY 50 scanning spectrophotometer was also used for routine measurements. Rate constants were determined by global analysis of the entire time dependent spectral data using the ReactLab Kinetics software.³³

High pressure experiments were carried out at pressures between 400-1600 atm, at different temperatures; the equipment has been described elsewhere.⁶¹ The concentration of $[\text{Cu}^{\text{II}}\text{LR}]^+$ was 1 mM. When studying the activation step of the atom transfer reaction (Eqn. 1), the concentration of initiator was 1 mM and the 2nd order rate constant was obtained from $k_{\text{obs}}/[\text{RX}]$ (see Results and Discussion). When studying the protonolysis reaction), the acid concentration was sufficiently high to reach k_{obs} saturation.

Synthesis

Acetonitrile- d_1

A mixture of $[\text{Cu}^{\text{II}}\text{LR}]^+$ (24.5 mg, 0.05 mmol) and D_2O (20 mg, 0.5 mmol) in 25 mL of dry CH_3CN were stirred overnight (open to air). After this time, the mixture became pale blue (initially, it was emerald green). The paramagnetic Cu(II) complex was removed from solution using a short silica column with compressed air. The ^2H NMR spectrum was recorded from the sample. ^2H -NMR (300 MHz): δ (ppm) 1.91 (t, 1H, $J = 2.3$ Hz).

Phenol- d_1

A slight modification on the method carried out by Caputo was followed.⁶² Recrystallized phenol (0.5 g, 5.3 mmol) was dissolved in 15 mL of dry THF and a cube of Na (1.0 g, 43.5 mmol) was carefully added. The solution was stirred overnight, after which the remaining Na cube was removed. Following this, the reaction was quenched with D_2O (15 mL), 10 drops of D_2SO_4 (96-98% in D_2O) were added, and the mixture was left stirring for 1 h. The deuterated phenol was then extracted with dry Et_2O , and a colorless solid was obtained after solvent evaporation and this was further dried under vacuum overnight (Yield: 89%, 0.45 g, 4.7 mmol). The compound was approx. 92% deuterated by NMR analysis. ^1H NMR (500 MHz, CDCl_3): 7.37-7.28 (m, 2H, Ph), 7.05 (t, $J = 7.12$ Hz, 1H, Ph), 6.98 (d, $J = 8.30$ Hz, 2H, Ph), 6.34 (s, OH). ^{13}C -NMR (125 MHz, CDCl_3): δ (ppm) 155.0, 130.0, 121.1, 115.3.

2-((2',2',6',6'-Tetramethylpiperidin-1'-oxy)acetonitrile (TEMPO- CH_2CN , TEMPO-R)

A mixture of de-aerated $[\text{Cu}^{\text{II}}\text{LR}]^+$ (50 mg, 0.1 mmol) and TEMPO (16 mg, 0.1 mmol) in 25 mL of dry CH_3CN were stirred overnight at 45 °C in a Schlenk tube. After this time, the colorless mixture was diluted with 20 mL of water and extracted with DCM (3×50 mL). The organic extracts were dried over MgSO_4 , and the solvent was evaporated to give a pale-yellow oil (17.5 mg, 90%). ^1H -NMR (500 MHz, CDCl_3): δ (ppm) 4.52 (s, 2H), 1.57-1.31 (m, 6H), 1.20 (s, 6H), 1.10 (s, 6H). ^{13}C -NMR (125 MHz, CDCl_3): δ (ppm) 116.2, 62.8, 60.5, 39.7, 33.1, 20.0, 17.0. LRMS (ESI) $[\text{M}+\text{H}]^+$: 196.92. Spectroscopic data matched the literature.⁶³

Associated Content

Supporting Information

Supporting Information is available from the Journal's website including NMR data, selected plots of the dependence of the observed rate constants on temperature and pressure. All the observed rate constants are also included in this document.

Author Information

Corresponding Authors

Paul V. Bernhardt

*Email: p.bernhardt@uq.edu.au

Manuel Martinez

*E-mail: manel.martinez@qi.ub.es

ORCID

Miguel A. González: 0000-0003-2396-8594

Craig M. Williams: 0000-0002-3834-7398

Manuel Martínez: 0000-0002-6289-4586

Paul V. Bernhardt: 0000-0001-6839-1763

Notes

The authors declare no competing financial interest

Acknowledgements

We gratefully acknowledge funding from the Australian Research Council (DP210102150) and the Ministerio de Ciencia e Innovación (PID2019-107006 GB-C21).

References

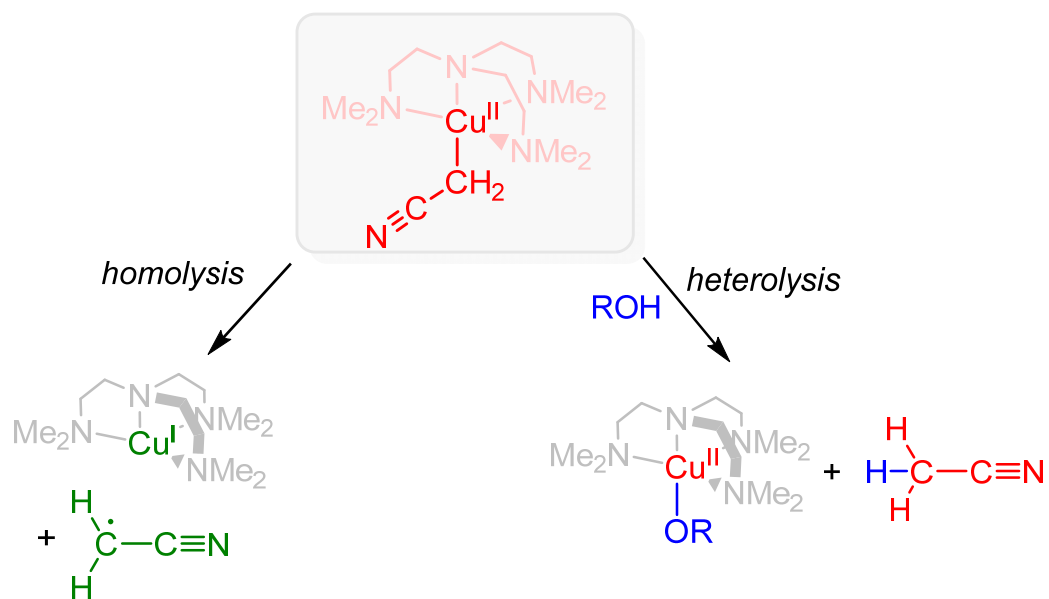
- (1) Crabtree, R. H. *The Organometallic Chemistry of the Transition Metals, Fourth Edition*. Wiley: 2005.
- (2) Poli, R. New Phenomena in Organometallic-Mediated Radical Polymerization (OMRP) and Perspectives for Control of Less Active Monomers. *Chem. Eur. J.* **2015**, *21*, 6988-7001.
- (3) Leifert, D.; Studer, A. The Persistent Radical Effect in Organic Synthesis. *Angew. Chem. Int. Ed.* **2020**, *59*, 74-108.
- (4) Elschenbroich, C. *Organometallics, 3rd, Completely Revised and Extended Edition*. Wiley-VCH: 2006.
- (5) Matyjaszewski, K. Atom Transfer Radical Polymerization (ATRP): Current Status and Future Perspectives. *Macromolecules* **2012**, *45*, 4015-4039.
- (6) Pintauer, T.; Matyjaszewski, K. Atom transfer radical addition and polymerization reactions catalyzed by ppm amounts of copper complexes. *Chem. Soc. Rev.* **2008**, *37*, 1087-1097.
- (7) Poli, R.; Shaver, M. P. Atom Transfer Radical Polymerization (ATRP) and Organometallic Mediated Radical Polymerization (OMRP) of Styrene Mediated by Diaminobis(phenolato)iron(II) Complexes: A DFT Study. *Inorg. Chem.* **2014**, *53*, 7580-7590.
- (8) Braunecker, W. A.; Brown, W. C.; Morelli, B. C.; Tang, W.; Poli, R.; Matyjaszewski, K. Origin of Activity in Cu-, Ru-, and Os-Mediated Radical Polymerization. *Macromolecules* **2007**, *40*, 8576-8585.
- (9) Allan, L. E. N.; MacDonald, J. P.; Nichol, G. S.; Shaver, M. P. Single Component Iron Catalysts for Atom Transfer and Organometallic Mediated Radical Polymerizations: Mechanistic Studies and Reaction Scope. *Macromolecules* **2014**, *47*, 1249-1257.
- (10) Zerk, T. J.; Bernhardt, P. V. Organo-Copper(II) Complexes as Products of Radical Atom Transfer. *Inorg. Chem.* **2017**, *56*, 5784-5792.
- (11) Zerk, T. J.; Gahan, L. R.; Krenske, E. H.; Bernhardt, P. V. The fate of copper catalysts in atom transfer radical chemistry. *Polymer Chem.* **2019**, *10*, 1460-1470.
- (12) González, M. A.; Harmer, J. R.; Bernhardt, P. V. Mapping the Pathway to Organocopper(II) Complexes Relevant to Atom Transfer Radical Polymerization. *Inorg. Chem.* **2021**, *60*, 10648-10655.
- (13) Kinoshita, I.; Wright, L. J.; Kubo, S.; Kimura, K.; Sakata, A.; Yano, T.; Miyamoto, R.; Nishioka, T.; Isobe, K. Design and synthesis of copper complexes of novel ligands based on the pyridine thiolate group. *Dalton Trans.* **2003**, 1993-2003.
- (14) Miyamoto, R.; Santo, R.; Matsushita, T.; Nishioka, T.; Ichimura, A.; Teki, Y.; Kinoshita, I. A complete series of copper(II) halide complexes (X = F, Cl, Br, I) with a novel Cu(II)-C(sp³) bond. *Dalton Trans.* **2005**, 3179-3186.
- (15) Tehranchi, J.; Donoghue, P. J.; Cramer, C. J.; Tolman, W. B. Reactivity of (Dicarboxamide)M^{II}-OH (M = Cu, Ni) Complexes – Reaction with Acetonitrile to Yield M^{II}-Cyanomethides. *Eur. J. Inorg. Chem.* **2013**, 2013, 4077-4084.
- (16) Zabawa, T. P.; Chemler, S. R. Copper(II) Carboxylate Promoted Intramolecular Diamination of Terminal Alkenes: Improved Reaction Conditions and Expanded Substrate Scope. *Org. Lett.* **2007**, *9*, 2035-2038.
- (17) Chemler, S. R.; Karyakarte, S. D.; Khoder, Z. M. Stereoselective and Regioselective Synthesis of Heterocycles via Copper-Catalyzed Additions of Amine Derivatives and Alcohols to Alkenes. *J. Org. Chem.* **2017**, *82*, 11311-11325.
- (18) Bunescu, A.; Ha, T. M.; Wang, Q.; Zhu, J. Copper-Catalyzed Three-Component Carboazidation of Alkenes with Acetonitrile and Sodium Azide. *Angew. Chem. Int. Ed.* **2017**, *56*, 10555-10558.
- (19) Wu, H.; Wang, Q.; Zhu, J. Copper-Catalyzed Enantioselective Domino Arylation/Semipinacol Rearrangement of Allylic Alcohols with Diaryliodonium Salts. *Chem. Eur. J.* **2017**, *23*, 13037-13041.
- (20) Lavernhe, R.; Torres-Ochoa, R. O.; Wang, Q.; Zhu, J. Copper-Catalyzed Aza-Sonogashira Cross-Coupling To Form Ynimines: Development and Application to the Synthesis of Heterocycles. *Angew. Chem. Int. Ed.* **2021**, *60*, 24028-24033.

- (21) De La Mare, H. E.; Kochi, J. K.; Rust, F. F. The oxidation and reduction of free radicals by metal salts. *J. Am. Chem. Soc.* **1963**, *85*, 1437-1449.
- (22) Cohen, H.; Meyerstein, D. Kinetics of reaction of copper(I) and copper(II) ions with 2,5-dioxacyclohexyl free radicals and homolysis of the aqua-copper(II)-2,5-dioxacyclohexyl complex in aqueous solutions. A pulse radiolysis study. *Inorg. Chem.* **1987**, *26*, 2342-2344.
- (23) Freiberg, M.; Mulac, W. A.; Schmidt, K. H.; Meyerstein, D. Reactions of aliphatic free radicals with copper cations in aqueous solutions. Part 3.—Reactions with cuprous ions: a pulse radiolysis study. *J. Chem. Soc., Faraday Trans.* **1980**, *76*, 1838-1848.
- (24) Meyerstein, D. Factors affecting the equilibrium constant of homolysis of complexes with metal-carbon σ bonds in aqueous solutions. Pulse radiolysis studies. *Pure Appl. Chem.* **1989**, *61*, 885-889.
- (25) Masarwa, M.; Cohen, H.; Saar, J.; Meyerstein, D. Metal Induced Decarboxylation of Aliphatic Free Radicals. I. Kinetics of the Reactions of Copper(I) and Copper(II) Ions with the 2-Methyl-2-Carboxylicacid-Propyl Free Radical in Aqueous Solutions. A Pulse Radiolysis Study. *Isr. J. Chem.* **1990**, *30*, 361-368.
- (26) Goldstein, S.; Czapski, G.; Cohen, H.; Meyerstein, D. Hydroxyl radical induced decarboxylation and deamination of 2-methylalanine catalyzed by copper ions. *Inorg. Chem.* **1992**, *31*, 2439-2444.
- (27) Ferraudi, G. Photochemical generation of metastable methylcopper complexes. Oxidation-reduction of methyl radicals by copper complexes. *Inorg. Chem.* **1978**, *17*, 2506-2508.
- (28) Fantin, M.; Lorandi, F.; Ribelli, T. G.; Szczepaniak, G.; Enciso, A. E.; Fliedel, C.; Thevenin, L.; Isse, A. A.; Poli, R.; Matyjaszewski, K. Impact of Organometallic Intermediates on Copper-Catalyzed Atom Transfer Radical Polymerization. *Macromolecules* **2019**, *52*, 4079-4090.
- (29) Thevenin, L.; Fliedel, C.; Matyjaszewski, K.; Poli, R. Impact of Catalyzed Radical Termination (CRT) and Reductive Radical Termination (RRT) in Metal-Mediated Radical Polymerization Processes. *Eur. J. Inorg. Chem.* **2019**, 2019, 4489-4499.
- (30) González, M. A.; Su, C.; Williams, C. M.; Bernhardt, P. V. Organocopper(II) complexes: new catalysts for carbon-carbon bond formation via electrochemical atom transfer radical addition (eATRA). *Chem. Sci.* **2022**, *13*, 10506-10511.
- (31) Ribelli, T. G.; Matyjaszewski, K.; Poli, R. The interaction of carbon-centered radicals with copper(I) and copper(II) complexes*. *J. Coord. Chem.* **2018**, *71*, 1641-1668.
- (32) Golubeva, E. N.; Gromov, O. I.; Zhidomirov, G. M. Cu(II)-Alkyl Chlorocomplexes: Stable Compounds or Transients? DFT Prediction of their Structure and EPR Parameters. *J. Phys. Chem. A* **2011**, *115*, 8147-8154.
- (33) Maeder, M.; King, P. *ReactLab Kinetics*, Jplus Consulting Pty Ltd, East Fremantle: WA, Australia, 2009.
- (34) Zhang, Q.; Wilson, P.; Li, Z.; McHale, R.; Godfrey, J.; Anastasaki, A.; Waldron, C.; Haddleton, D. M. Aqueous Copper-Mediated Living Polymerization: Exploiting Rapid Disproportionation of CuBr with Me₆TREN. *J. Am. Chem. Soc.* **2013**, *135*, 7355-7363.
- (35) Levere, M. E.; Nguyen, N. H.; Sun, H.-J.; Percec, V. Interrupted SET-LRP of methyl acrylate demonstrates Cu(0) colloidal particles as activating species. *Polymer Chem.* **2013**, *4*, 686-694.
- (36) Enayati, M.; Jezorek, R. L.; Smail, R. B.; Monteiro, M. J.; Percec, V. Ultrafast SET-LRP in biphasic mixtures of the non-disproportionating solvent acetonitrile with water. *Polymer Chem.* **2016**, *7*, 5930-5942.
- (37) Lligadas, G.; Rosen, B. M.; Monteiro, M. J.; Percec, V. Solvent Choice Differentiates SET-LRP and Cu-Mediated Radical Polymerization with Non-First-Order Kinetics. *Macromolecules* **2008**, *41*, 8360-8364.
- (38) Rosen, B. M.; Jiang, X.; Wilson, C. J.; Nguyen, N. H.; Monteiro, M. J.; Percec, V. The disproportionation of Cu(I)X mediated by ligand and solvent into Cu(0) and Cu(II)X₂ and its implications for SET-LRP. *J. Polym. Sci., Part A: Polym. Chem.* **2009**, *47*, 5606-5628.
- (39) Fischer, H. The Persistent Radical Effect: A Principle for Selective Radical Reactions and Living Radical Polymerizations. *Chem. Rev.* **2001**, *101*, 3581-3610.
- (40) Johnston, L. J.; Tencer, M.; Scaiano, J. C. Evidence for hydrogen transfer in the photochemistry of 2,2,6,6-tetramethylpiperidine N-oxyl. *J. Org. Chem.* **1986**, *51*, 2806-2808.

- (41) Kryszewski, P.; Matyjaszewski, K. Kinetics of Atom Transfer Radical Polymerization. *Eur. Polym. J.* **2017**, *89*, 482-523.
- (42) Tang, W.; Kwak, Y.; Braunecker, W.; Tsarevsky, N. V.; Coote, M. L.; Matyjaszewski, K. Understanding Atom Transfer Radical Polymerization: Effect of Ligand and Initiator Structures on the Equilibrium Constants. *J. Am. Chem. Soc.* **2008**, *130*, 10702-10713.
- (43) Halpern, J. Determination and significance of transition metal-alkyl bond dissociation energies. *Acc. Chem. Res.* **1982**, *15*, 238-244.
- (44) Endicott, J. F.; Ferraudi, G. J. A flash photolytic investigation of low energy homolytic processes in methylcobalamin. *J. Am. Chem. Soc.* **1977**, *99*, 243-245.
- (45) Poli, R. A journey into metal-carbon bond homolysis. *Compt. Rend. Chim.* **2021**, *24*, 147-175.
- (46) Li, G.; Zhang, F. F.; Chen, H.; Yin, H. F.; Chen, H. L.; Zhang, S. Y. Determination of Co-C bond dissociation energies for organocobalt complexes related to coenzyme B12 using photoacoustic calorimetry. *J. Chem. Soc., Dalton Trans.* **2002**, 105-110.
- (47) Berger, J.; Kotowski, M.; Van Eldik, R.; Frey, U.; Helm, L.; Merbach, A. E. Kinetics and mechanism of solvent-exchange and anation reactions of sterically hindered diethylenetriamine complexes of palladium(II) in aqueous solution. *Inorg. Chem.* **1989**, *28*, 3759-3765.
- (48) Navon, N.; Golub, G.; Cohen, H.; Meyerstein, D. Kinetics and Reaction Mechanisms of Copper(I) Complexes with Aliphatic Free Radicals in Aqueous Solutions. A Pulse-Radiolysis Study. *Organometallics* **1995**, *14*, 5670-5676.
- (49) Chiarotto, I.; Mattiello, L.; Feroci, M. The Electrogenerated Cyanomethyl Anion: An Old Base Still Smart. *Acc. Chem. Res.* **2019**, *52*, 3297-3308.
- (50) Thaler, F.; Hubbard, C. D.; Heinemann, F. W.; van Eldik, R.; Schindler, S.; Fábán, I.; Dittler-Klingemann, A. M.; Hahn, F. E.; Orvig, C. Structural, Spectroscopic, Thermodynamic and Kinetic Properties of Copper(II) Complexes with Tripodal Tetraamines. *Inorg. Chem.* **1998**, *37*, 4022-4029.
- (51) Bakac, A.; Butkovic, V.; Espenson, J. H.; Orhanovic, M. Concurrent homolysis, β -elimination, and hydrolysis of macrocyclic alkylchromium complexes. *Inorg. Chim. Acta* **2000**, *300-302*, 280-284.
- (52) Shi, S.; Espenson, J. H.; Bakac, A. Organochromium(III) macrocyclic complexes. Factors controlling homolytic vs heterolytic cleavage of the chromium carbon bond. *Inorg. Chem.* **1990**, *29*, 4318-4322.
- (53) Espenson, J. H. Homolytic and Free Radical Pathways in the Reactions of Organochromium Complexes. In *Progr. Inorg. Chem.*, 1983; pp 189-212.
- (54) Wilkins, R. G. *Kinetics and mechanisms of reactions of transition metal complexes*. 2nd Thoroughly Revised Edition ed.; VCH Publishers: New York, N. Y., 1991.
- (55) Lappin, A. G. *Redox Mechanisms in Inorganic Chemistry*. Ellis Horwood: 1994.
- (56) González, G.; Martínez, M.; Rodríguez, E. Effect of amine substituents and neutral leaving groups on the activation volume for aquation of octahedral pentaamine complexes of Cr and Rh. *J. Chem. Soc., Dalton Trans.* **1995**, 891-892.
- (57) Martínez, M.; Pitarque, M.-A.; van Eldik, R. Outer-sphere redox reactions of $[\text{Co}^{\text{III}}(\text{NH}_3)_5(\text{H}_x\text{P}_y\text{O}_z)]^{(m-3)-}$ complexes. A temperature- and pressure-dependence kinetic study on the influence of the phosphorus oxoanions. *J. Chem. Soc., Dalton Trans.* **1996**, 2665-2671.
- (58) Granell, J.; Martínez, M. Kinetic-mechanistic studies of cyclometalating C-H bond activation reactions on Pd(II) and Rh(II) centres: The importance of non-innocent acidic solvents in the process. *Dalton Trans.* **2012**, *41*, 11243-11258.
- (59) Laga, E.; García-Montero, A.; Sayago, F. J.; Soler, T.; Moncho, S.; Catiuela, C.; Martínez, M.; Urriolabeitia, E. P. Cyclopalladation and Reactivity of Amino Esters through C-H Bond Activation: Experimental, Kinetic, and Density Functional Theory Mechanistic Studies. *Chem. - Eur. J.* **2013**, *19*, 17398-17412.
- (60) Bjelopetrović, A.; Barišić, D.; Duvnjak, Z.; Džajić, I.; Juribašić Kulcsár, M.; Halasz, I.; Martínez, M.; Budimir, A.; Babić, D.; Čurić, M. A Detailed Kinetic-Mechanistic Investigation on the Palladium C-H Bond Activation in Azobenzenes and Their Monopalladated Derivatives. *Inorg. Chem.* **2020**, *59*, 17123-17133.
- (61) Bernhardt, P. V.; Gonzalez, M. A.; Martinez, M. Kinetic-mechanistic Study on the Oxidation of Biologically Active Iron(II) Bis(thiosemicarbazone) Complexes by Air. Importance of

- NH \cdots O $_2$ Interactions As Established by Activation Volumes. *Inorg. Chem.* **2017**, 56, 14284-14290.
- (62) Bentley, J. N.; Caputo, C. B. Catalytic Hydroarylation of Alkenes with Phenols using B(C $_6$ F $_5$) $_3$. *Organometallics* **2018**, 37, 3654-3658.
- (63) Bunescu, A.; Wang, Q.; Zhu, J. Copper-Mediated/Catalyzed Oxyalkylation of Alkenes with Alkynitriles. *Chem. Eur. J.* **2014**, 20, 14633-14636.

TOC Graphic



Dissociation of the C-bound cyanomethyl ligand from a Cu(II) tetraamine has been shown to occur via spontaneous Cu^{II}-C bond homolysis releasing a radical and Cu(I). However, in the presence of a weak Brønsted acid (ROH), Cu^{II}-C bond heterolysis is observed forming Cu^{II}-OR as the product.